Abl Tyrosine Kinase Promotes Dorsal Ruffles but Restrains Lamellipodia Extension during Cell Spreading on Fibronectin

Hua Jin* and Jean Y.J. Wang*†‡

*Division of Biological Sciences, †Division of Hematology-Oncology, Department of Medicine, School of Medicine, and ‡Moores Cancer Center, University of California, San Diego, La Jolla, CA 92093-0820

The nonreceptor Abl tyrosine kinase stimulates F-actin microspikes and membrane ruffles in response to adhesion and growth factor signals. We show here that induced dimerization of Abl-FKBP, but not the kinase-defective AblKD-FKBP, inhibits cell spreading on fibronectin. Conversely, knockdown of cellular Abl by shRNA stimulates cell spreading. The Abl kinase inhibitor, imatinib, also stimulates cell spreading and its effect is overridden by the imatinib-resistant AblT315I. Expression of Abl but not AbkKD in *Abl/Arg*-deficient cells again inhibits spreading. Furthermore, Abl inhibits spreading of cells that express the activated Rac, RacV12, correlating with RacV12 localization to dorsal membrane protrusions. Ectopic expression of CrkII, a Rac activator that is inactivated by Abl-mediated tyrosine phosphorylation, antagonizes Abl-mediated dorsal membrane localization of RacV12. Ectopic expression of a dynamin-2 mutant, previously shown to induce Rac-GTP localization to the dorsal membrane, abolishes the stimulatory effect of imatinib on cell spreading. These results suggest that Abl tyrosine kinase, through CrkII phosphorylation and in collaboration with dynamin-2 can regulate the partitioning of Rac-GTP to favor dorsal ruffles during cell spreading. The Abl-dependent dorsal membrane localization of activated Rac explains its positive role in ruffling and negative role in cell spreading and migration.

INTRODUCTION

The *Abl* gene is present in the genomes of multicellular eukaryotes from *Caenorhabditis elegans* to human and encodes a nonreceptor tyrosine kinase with a conserved actin-binding domain (McWhirter and Wang, 1993; Van Etten *et al.,* 1994; Woodring *et al.,* 2003; Hantschel *et al.,* 2005; Wiesner *et al.,* 2005). The mammalian Abl tyrosine kinase is constitutively expressed and essential to the proper development as the knockout of mouse *Abl* gene causes neonatal lethality (Schwartzberg *et al.,* 1991; Tybulewicz *et al.,* 1991). An *Abl*-related gene (*Arg*) is also present in the mammalian genome; although the knockout of *Arg* did not cause developmental defects, the combined ablation of *Abl* and *Arg* leads to early embryonic lethality (Koleske *et al.,* 1998). The Abl tyrosine kinase undergoes nucleocytoplasmic shuttling and plays an important role in the regulation of cell growth and cell death (Wang, 2000; Zhu and Wang, 2004). The conserved interaction between Abl and actin suggests the regulation of actin dynamics to be a key function of this tyrosine kinase (Woodring *et al.,* 2003). Indeed, the Abl tyrosine kinase is found to stimulate dorsal ruffles in response to growth factors such as platelet-derived growth factor (PDGF) and epidermal growth factor (EGF; Plattner *et*

Address correspondence to: Jean Y.J. Wang (jywang@ucsd.edu).

Abbreviations used: ECM, extracellular matrix; Arg, Abl-related gene; DKO, double knockout; FN, fibronectin; wt, wild type; dyn, dynamin.

al., 1999; Sini *et al.,* 2004). Abl kinase is also activated by cell adhesion to stimulate the formation of F-actin microspikes (Lewis *et al.,* 1996; Woodring *et al.,* 2002).

Dorsal ruffles and microspikes are formed as a result of regulated actin polymerization at the plasma membrane. The ability of Abl kinase to promote actin polymerization is suggested by the findings that Abl phosphorylates components of the WAVE complex, including Abi-1/2 and WAVE2 (Dai and Pendergast, 1995; Fan and Goff, 2000; Leng *et al.,* 2005; Stuart *et al.,* 2006). The WAVE complex is composed of WAVE1/2, Abi1/2, NAP1, SRA, and HSPC300 subunits (Eden *et al.,* 2002; Innocenti *et al.,* 2004). The WAVE complex can be activated by Rac-GTP binding the SRA, or NCK binding the NAP1 subunit (Cory and Ridley, 2002; Eden *et al.,* 2002; Steffen *et al.,* 2004). Activated WAVE complex stimulates Arp2/3 to nucleate actin polymerization (Takenawa and Miki, 2001; Stradal *et al.,* 2004; Soderling and Scott, 2006). Abl-mediated tyrosine phosphorylation of WAVE2 is associated with an enhanced stimulation of the Arp2/3 complex and increased membrane ruffles (Leng *et al.,* 2005; Stuart *et al.,* 2006). Activated Abl tyrosine kinase also phosphorylates the Dok-1 adaptor protein to recruit Nck-family of adaptors, leading to Rac-GTP-independent formation of F-actin microspikes (Woodring *et al.,* 2002; Woodring *et al.,* 2004). These results establish Abl as a positive effector in transducing growth factor and cell adhesion signals to the stimulation of actin polymerization.

Paradoxically, Abl tyrosine kinase inhibits cell migration, a process that is also dependent on actin polymerization (Suetsugu and Takenawa, 2003). Inhibition of Abl tyrosine kinase stimulates the migratory response of carcinoma cells to hepatocyte growth factor (Frasca *et al.,* 2001). Ectopic expression of Abl tyrosine kinase in Cos1 or *Abl/Arg* double

knockout cells inhibits cell migration (Kain and Klemke, 2001). During migration, cells form lamellipodia at the leading edge (Small *et al.*, 2002). This process of lamellipodia extension also promotes cell spreading on extracellular matrix (ECM) proteins such as fibronectin (Price *et al.*, 1998). The small GTPase Rac is essential for lamellipodia formation in migratory and spreading cells (Ridley *et al.*, 1999, 2003). Ectopic expression of a dominant negative Rac mutant, RacN17, inhibits lamellipodia extension and cell spreading (Clark *et al.*, 1998; Price *et al.*, 1998). Fibroblasts derived from *Rac1* knockout mouse embryos spread slower than the *Rac1* wild-type (wt) cells due to the deficiency in lamellipodia formation (Vidali *et al.*, 2006).

Abl has been reported to exert positive and negative effects on Rac. The oncogenic v-Abl tyrosine kinase stimulates Rac and Rac-dependent pinocytosis to promote cell proliferation (Renshaw *et al.*, 1996). The cellular Abl tyrosine kinase is activated by growth factors such as PDGF and EGF to increase the levels of Rac-GTP and stimulate membrane ruffling (Sini *et al.*, 2004). On the other hand, Abl-dependent tyrosine phosphorylation of Crk has also been shown to disrupt the Crk-Cas complex, correlating with a reduction of Rac-GTP level and the inhibition of cell migration (Kain and Klemke, 2001).

Previous studies have established that Abl kinase is activated upon cell adhesion to ECM proteins such as fibronectin (Lewis *et al.*, 1996; Lewis and Schwartz, 1998; Woodring *et al.*, 2001; Woodring *et al.*, 2002; Woodring *et al.*, 2005). Abl activity peaks between 15 and 25 min after plating cells onto fibronectin-coated surface and returns to a basal level that is higher in attached than detached cells (Lewis *et al.*, 1996; Lewis and Schwartz, 1998; Woodring *et al.*, 2001, 2002, 2005). We show here that Abl tyrosine kinase exerts a negative role in cell spreading, consistent with its inhibitory effect on cell migration (Frasca *et al.*, 2001; Kain and Klemke, 2001). Furthermore, we show that Abl kinase inhibits the spreading of cells that express the constitutively active RacV12 protein. The Abl kinase caused preferential localization of RacV12 to dorsal membrane protrusions. Ectopic expression of CrkII, antagonizes Abl-mediated dorsal membrane localization of RacV12 and reduced Abl-mediated inhibition of cell spreading. Ectopic expression of a dynamin mutant, previously shown to induce Rac-GTP localization to the dorsal membrane, abolishes the stimulatory effect of imatinib on cell spreading. Our findings suggest that Abl kinase-dependent dorsal membrane sequestration of Rac-GTP may reduce the pool of Rac-GTP for lamellipodia formation at the leading edge and thus account for Abl-dependent inhibition of cell spreading and migration.

MATERIALS AND METHODS

DNA Constructs, Transfection, and Retroviral Infection

Abl-FKBP and the AblKD-FKBP coding sequence was released from pC4M-Fv2E vector (Vella *et al.*, 2003) by XbaI and BamHI digestion and blunt-end ligated into PMSCVhyg (Clontech, Palo Alto, CA) at the XhoI site. The wt-Abl (murine type IV), AblT315I, and AblKD were ligated into PMSCVhyg at the SalI site. The Phoenix retroviral expression system (Orbigen, San Diego, CA) was used to produce recombinant retrovirus. Hemagglutinin (HA)-RacV12 and green fluorescent protein (GFP)-Rac (gifts of Mark H. Ginsberg, UCSD, La Jolla, CA), GFP-RacV12 (a gift of Martin A. Schwartz, University of Virginia, Charlottesville, VA), myc-CrkII and myc-CrkI-Y221F (gifts of Kritiina Vuori, The Burnham Institute, La Jolla, CA), and HA-dynamin-2 and HA-dynamin-2-K44A (gifts of Sandra L. Schmid, The Scripps Research Institute, La Jolla, CA) were transfected using Lipofectamine 2000 (Invitrogen, Carlsbad, CA). Stable polyclonal 3T3/Abl-FKBP, 3T3/AblKD-FKBP, 3T3/FKBP, *Abl/Arg* DKO/vector, *Abl/Arg* DKO/Abl, and *Abl/Arg* DKO/AblKD were selected by hygromycin resistance after infection with the pMSCVhyg retroviruses.

Short Hairpin RNA Knockdown

Targeting sequences against LacZ and Abl were AACAGTTGCGCAGCCT-GAATG and AACCTGTACACTTTCTGTGTG, respectively. Pairs of complementary oligonucleotides were annealed and ligated into HindIII/BglII-digested pRS short hairpin RNA (shRNA) expression retrovirus vector (Brummelkamp *et al.*, 2002). The phoenix retroviral expression system (Orbigen) was used to produce shRNA expression virus. Stable polyclonal LacZ and Abl knockdown cell lines were selected by puromycin resistance.

Cell Culture and Reagents

NIH3T3 fibroblasts and *Abl/Arg* double 6 knockout fibroblasts were cultured in DMEM, supplemented with 10% fetal bovine serum (Hyclone, Logan, UT) and antibiotics. Dimerizer, AP20187 (ARIAD, Cambridge, MA) was used at 50 nM. Imatinib was used at 5 μM. Coverslides were coated with fibronectin at 10 μg/ml at 4°C overnight.

Cell Spreading Assays and Immunofluorescence

Cells of ~80% confluence were trypsinized, resuspended in serum-free DMEM containing 0.5 mg/ml soybean trypsin inhibitor, and washed twice with serum-free DMEM/0.1% BSA. Cells were held in suspension in DMEM/0.1% bovine serum albumin (BSA) for 45–75 min at room temperature and then plated on fibronectin-coated coverslides and allowed to spread at 37°C. At various time points, cells were fixed in 4% paraformaldehyde, permeabilized in 0.3% Triton X-100/phosphate-uffered saline (PBS), blocked in 10% goat serum/PBS, and then stained with monoclonal anti-Abl 8E9 (BD Biosciences, San Jose, CA) followed by Alexa 568–conjugated secondary antibody and/or Alexa 546– or 488–conjugated phalloidin (Molecular Probes, Eugene, OR). Fluorescent images were captured with a CCD camera. The surface areas of cells were measured with Image-Pro Software (Media Cybernetics, Carlsbad, CA). At least 100 cells were analyzed per sample. Results were from three independent experiments.

Adhesion Assay

Plates (96-well) were coated with fibronectin at concentrations of 0.1 to 20 μg/ml. Suspension cells were prepared as in the spreading experiments, seeded at 1×10^4 cells per well, and allowed to adhere for 5–120 min at 37°C. Wells were washed twice with serum-free DMEM/0.1% BSA, and adherent cells were fixed with 5% glutaraldehyde and then stained with crystal violet (0.1%). After extensive washing to remove the free dye, the cell-bound crystal violet was extracted with 0.5% Triton X-100, and absorbance was measured at 595 nm.

Rac-GTP and Rho GTP Pulldown Assay

Suspension cells were prepared as in spreading experiments and were allowed to spread on fibronectin-coated six-well plates for the indicated time. Cells were lysed on plates in the presence of glutathione *S*-transferase (GST)-PBD (Pak Rac-binding domain). Rac-GTP was pulled down with bacteria-purified GST-PBD as described (Azim *et al.*, 2000). Rho-GTP was pulled down with bacteria-purified GST-RBD (Rhotekin Rho binding domain; Hall and Nobes, 2000). X-ray films of the immunoblotting experiments were scanned, and digital signals were quantitated with Chemilmager 4400 software (Alpha Innotech, San Leandro, CA).

Immunoprecipitation, Immunoblotting, and Antibodies

Cells were lysed in RIPA buffer (50 mM Tris, pH 7.4, 150 mM NaCl, 1% Triton X-100, 0.5% deoxycholate, 0.1% SDS, protease inhibitor cocktail [Roche, Indianapolis, IN], 1 mM phenylmethylsulfonyl fluoride, 1 mM EDTA, 10 mM sodium vanadate, and 10 mM β-glycerol-phosphate). Whole cell lysate (50 μg) was fractionated on SDS-PAGE, transferred to nitrocellulose membrane, and blotted with primary antibodies, followed by horseradish peroxidase–conjugated secondary antibodies, and visualized by chemiluminescence. For immunoprecipitation, 1 mg of cell lysate was used. Antibodies used were as follows: anti-Abl, 8E9 (BD Biosciences, San Jose, CA), anti-phosphotyrosine, 4G10 (Upstate Biotechnology, Lake Placid, NY), anti-tubulin (Santa Cruz Biotechnology, Santa Cruz, CA), anti-HA (Covance, Madison, WI), anti-GFP (Clontech), anti-Rac1 (Stratagene, La Jolla, CA), anti-RhoA (Santa Cruz Biotechnology), anti-dok-1 (Santa Cruz Biotechnology), and anti-actin (Sigma, St. Louis, MO).

Microscopy

Fluorescent images were obtained with a fluorescence microscopy (Zeiss, Thornwood, NY) or a delta vision deconvolution microscope system (Nikon TE-200 microscope, Melville, NY). SEM images were obtained with a Hitachi S-2700 scanning electron microscope (Hitachi High-Technologies, San Jose, CA).

Quantitation of Dorsal Localization of RacV12 and F-actin

The localization of GFP-RacV12, GFP-Rac, and GFP was examined in fully spread cells by deconvolution microscopy. Dorsal membrane protrusions are mostly absent from fully spread 3T3/vector cells. With 3T3/Abl cells that

overexpressed Abl, prominent dorsal membrane protrusions with GFP-signals were observed in fully spread cells. Therefore, we made a binary distinction between cells with GFP signals in dorsal membrane protrusions (of various degrees) and cells without GFP signals in dorsal membrane protrusions. A similar binary distinction was applied to the quantitation of dorsal F-actin ruffles. The percentage of cells with or without dorsal F-actin ruffles was determined by examining at least 50 cells for each sample from three independent experiments. For experiments in Figure 7E, 3T3 cells plated in the presence or absence of imatinib were allowed to spread for 20 or 40 min, fixed, and stained with Alexa-546–conjugated phalloidin. Individual cells were analyzed for size and dorsal F-actin protrusions. Cells were grouped into 11 categories based on size, and in each category, at least 50 cells were counted to determine the percentage of cells with dorsal F-actin ruffles.

RESULTS

Dimerization of Abl-FKBP Inhibits Cell Spreading on Fibronectin

We generated an Abl-FKBP, as well as an Abl kinase defective-FKBP (AblKD-FKBP) fusion protein and adopted the strategy of activating Abl kinase activity with a chemical inducer of dimerization (Smith and Van Etten, 2001; Vella et al., 2003). Previous studies have shown that in the presence of a bivalent FKBP ligand, FKBP-Abl or Abl-FKBP undergoes dimerization leading to its autophosphorylation and kinase activation (Smith and Van Etten, 2001; Vella et al., 2003). The Abl-FKBP and AblKD-FKBP used in this study was constructed by fusing two copies of FKBPv, a variant of FKBP that specifically interacts with a synthetic ligand, AP20187 (Clackson et al., 1998), and the HA epitope to the C-terminus of Abl (murine type IV; Figure 1A). The Abl-FKBP or AblKD-FKBP fusion cassette was then introduced into an MSCV-based retroviral vector for the production of

recombinant retroviruses, which were used to infect mouse 3T3 fibroblasts and to establish polyclonal cell lines stably expressing Abl-FKBP, AblKD-FKBP, or FKBP (3T3/Abl-FKBP, 3T3/AblKD-FKBP, and 3T3/FKBP). The level of Abl-FKBP and AblKD-FKBP in 3T3/Abl-FKBP and 3T3/AblKD-FKBP cells was comparable to that of endogenous Abl (Figure 1B). The Abl-FKBP protein contained basal tyrosine phosphorylation in the absence of AP20187 (Figure 1B). After the addition of dimerizer, we observed a further approximate twofold increase in Abl-FKBP tyrosine phosphorylation (Figure 1B), confirming that inducing Abl-FKBP dimerization elevated its kinase activity (Smith and Van Etten, 2001; Vella et al., 2003). As a control, the AblKD-FKBP protein did not contain detectable tyrosine phosphorylation in the absence or presence of dimerizer (Figure 1B).

To examine the effect of Abl-FKBP dimerization on cell spreading, exponentially growing cells were trypsinized and then treated with dimerizer (or vehicle control) while they were held in suspension in serum-free media. After a 30-min preincubation with dimerizer, cells were plated on fibronectin-coated coverslides, allowed to spread under serum-free condition, and then collected for image analyses after staining with fluorescently labeled phalloidin. Dimerizer treatment did not change the spreading of control 3T3/FKBP cells (Figure 1C), as measured by either cell surface area (Figure 1D) or percentage of spread cells (Figure 1E). The spreading of 3T3/Abl-FKBP cells were reduced when compared with the 3T3/FKBP cells even in the absence of dimerizer (Figure 1, C–E). With dimerizer treatment, the spreading of 3T3/Abl-FKBP cells was further decreased (Figure 1,

Figure 1. Dimerization of Abl-FKBP causes slower cell spreading on fibronectin. (A) Diagram of Abl (murine type IV) and Abl-FKBP fusion proteins. PTK, protein tyrosine kinase domain; NLS, nuclear localization signal; NES, nuclear export signal; FABD, F-actin binding domain; FKBPv, modified FK506 binding domain (Clackson et al., 1998). The kinase defective mutant (KD) was created by substitution of Lys 295 with His (Welch and Wang, 1995). (B) The indicated cells were detached, held in suspension for 45 min in serum-free DMEM, and then treated with AP20187 (50 nM) or vehicle (0.1% ethanol) for 30 min. Cells were harvested for immunoprecipitation (IP) and immunoblotting (WB) with indicated antibodies as described in Materials and Methods. (C) The indicated cells were treated with AP20187 or vehicle as in B. Cells were fixed 40 min after plated on FN (10 μg/ml)-coated slides and stained with Alexa 546–conjugated phalloidin. Scale bars equal 50 μm. (D) Quantitation of cell spreading in C by measuring cell surface area shown as box plots with the minimum, the median, the maximum, the 25th and the 75th percentile values. Values shown are from at least 100 cells for each sample. (E) Quantitation of cell spreading in (C) by counting the number of spread cells (marked by arrows in C) among at least 100 cells. The values and standard deviations were from three independent experiments.
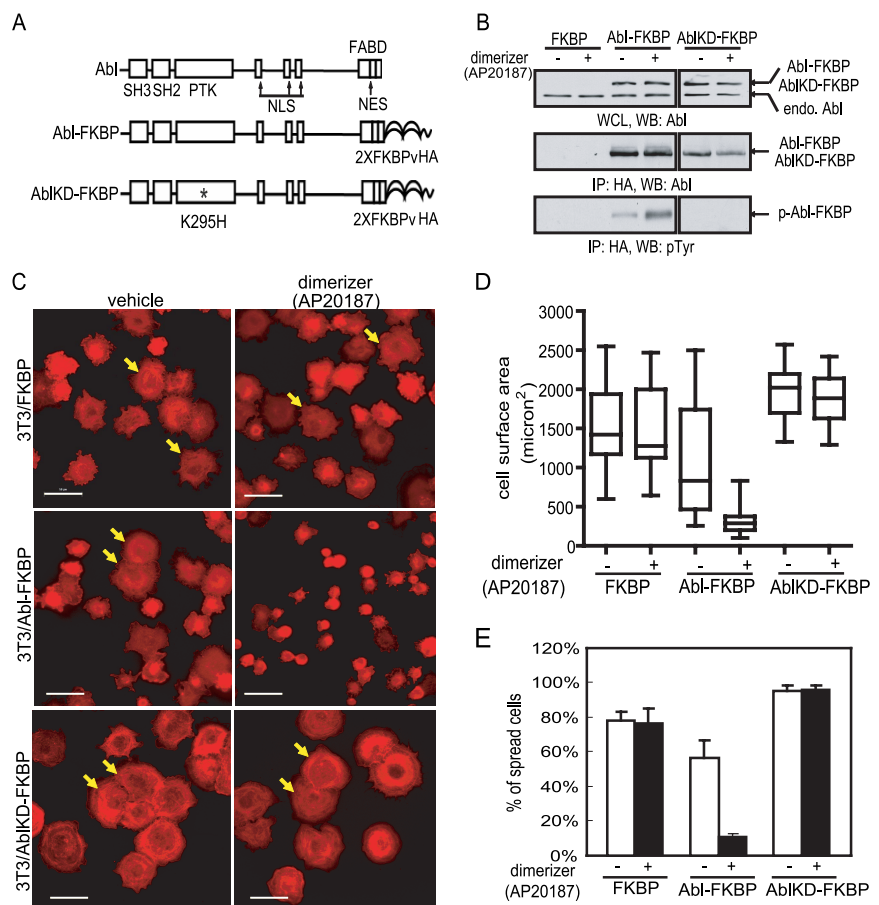
C–E). By contrast, the spreading of 3T3/AblKD-FKBP cells was increased relative to 3T3/FKBP cells in the absence of dimerizer (Figure 1, C–E). Furthermore, dimerizer treatment did not alter the spreading of 3T3/AblKD-FKBP cells (Figure 1, C–E). Thus, dimerization-induced activation of Abl-FKBP kinase caused a reduction in cell spreading on fibronectin.
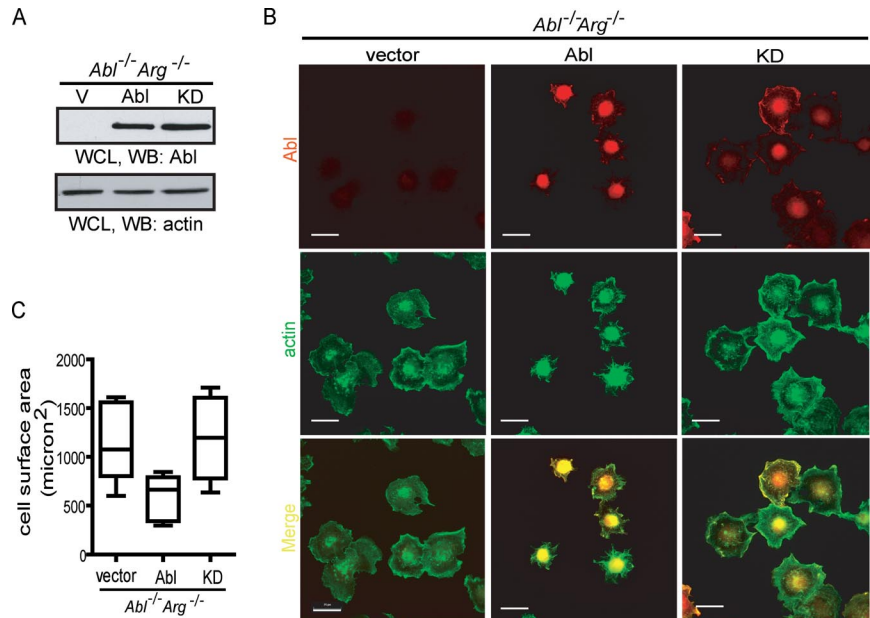
Inhibition of Endogenous Abl Kinase Promotes Cell Spreading

Abl kinase is transiently activated upon cell adhesion to fibronectin (Lewis *et al.*, 1996; Lewis and Schwartz, 1998; Woodring *et al.*, 2002). To examine if endogenous Abl also inhibits cell spreading, we stably expressed *Abl-shRNA* (3T3/Abl-shRNA) to reduce its levels by about twofold (Figure 2B). We found the 3T3-*Abl-shRNA* cells to spread faster than 3T3/*LacZ-shRNA* cells (Figure 2, A and B), consistent with Abl being a negative effector in cell spreading. We also performed spreading experiments with 3T3 cells in the pres-ence or absence of an Abl kinase inhibitor, imatinib (Gleevec, Novartis, Stein, Switzerland; Druker *et al.*, 1996; Schindler *et al.*, 2000). Cells treated with imatinib consis-tently spread faster than those treated with vehicle control (Figure 2, A and B). To demonstrate that the effect of ima-tinib was due to the inhibition of Abl kinase, we used an imatinib-resistant Abl kinase, AblT315I, which was con-structed based on the mutation identified in a imatinib-resistant BCR-ABL kinase (Gorre *et al.*, 2001). Wild-type murine Abl and its 315I derivative (AblT315I) were ex-pressed in 3T3 fibroblasts via retroviral-mediated gene transfer. Cell spreading and immunoblotting experiments were performed 48 h after infection to ensure high levels of ectopic Abl and AblT315I expression (Figure 2C). By mea-suring the phosphotyrosine content of Dok-1, a known sub-strate of Abl kinase (Woodring *et al.*, 2002), we confirmed that AblT315I activity was resistant to imatinib (Figure 2C). Cells expressing ectopic wt-Abl (3T3/Abl) spread slower than those infected with retroviral vector (3T3/vector), but
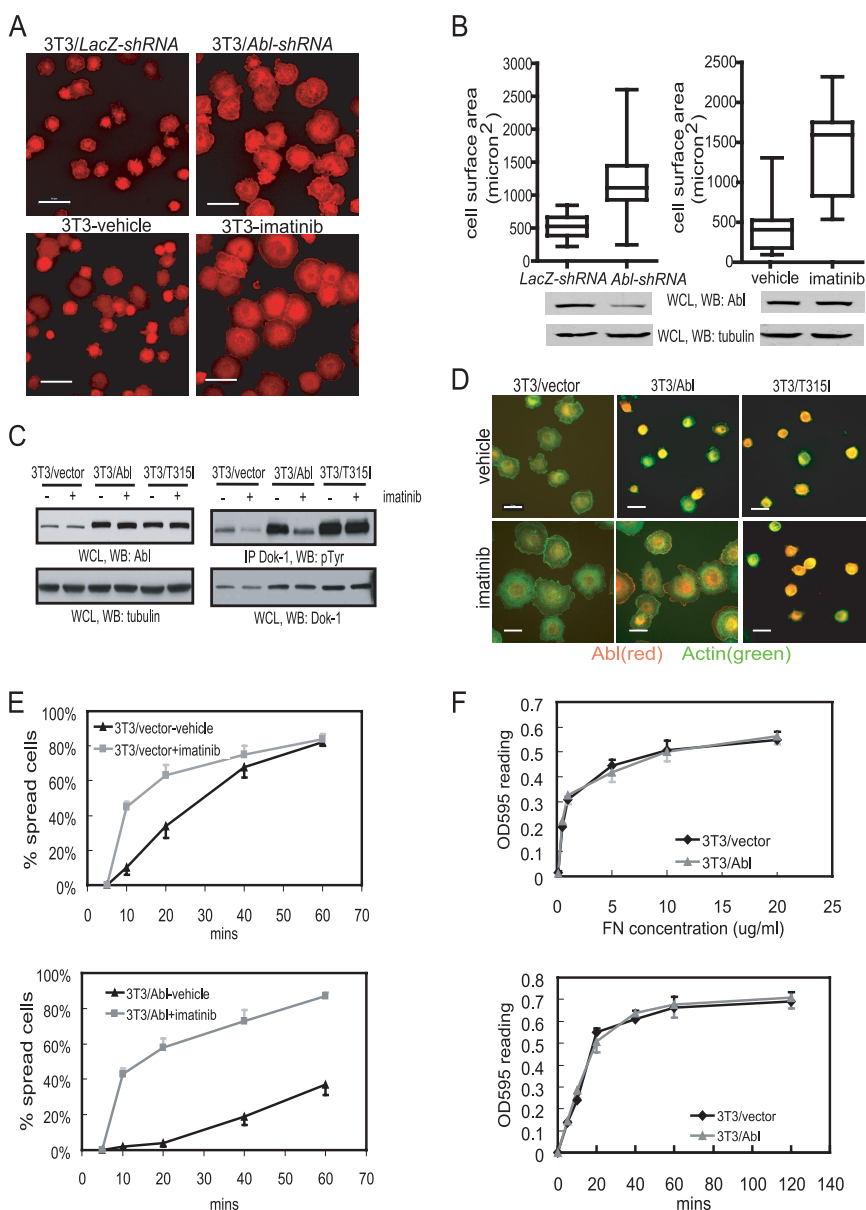
Figure 2. Knockdown of Abl or inhibition of Abl kinase by imatinib promotes cell spread-ing. (A6) Top left panel: 3T3 cells stably ex-pressing LacZ shRNA; top right panel: 3T3 cells stably expressing Abl shRNA. Bottom left panel, 3T3 cells treated with vehicle; bottom right panel, 3T3 cells treated with imatinib (5 μM). The indicated cells were detached and held in suspension for 30 min in serum-free DMEM, and then treated with imatinib (5 μM) or vehicle (0.1% DMSO) for 45 min before plating on FN (10 μg/ml)-coated coverslides. Cells were fixed 20 min later and stained with Alexa 546–conjugated phalloidin. Scale bars, 50 μm. (B) Quantitation of cell spreading in (A) by measuring cell surface area shown as box plots. Values shown are from at least 100 cells for each sample. (C) 3T3 cells were in-fected with retrovirus encoding vector, Abl, or Abl315I, treated with imatinib or vehicle as in (A) 48 h after infection, and then harvested for immunoblotting (WB) and immunoprecipita-tion (IP) with the indicated antibodies. (D) Cells in C were fixed 20 min after plated on FN-coated coverslides and then stained with anti-Abl/Alexa 568– conjugated secondary antibody (red) and Alexa 488–conjugated phalloidin (green). Scale bars, 25 μm. (E) The indicated cells treated with imatinib or vehicle as in A were plated on FN-coated coverslides, fixed at the indicated time, and the percentage of spread cells determined. In the 3T3/Abl sample, only cells with increased anti-Abl im-munofluorescence signal were scored. At least 100 cells were counted in each sample from three independent experiments. (F) The 3T3/vector or 3T3/Abl cells were detached and replated on fibronectin. Cell adhesion was measured at the indicated time after plating on 10 μg/ml fibronectin, or at 1 h after plating cells on different concentrations of FN (0, 0.1, 0.5, 1, 5, 10, and 20 μg/ml) as described in *Materials and Methods*.

A

$Abl^{-/-} Arg^{-/-}$

V Abl KD

WCL, WB: Abl

WCL, WB: actin

B

$Abl^{-/-}Arg^{-/-}$

vector   Abl   KD

Abl

actin

Merge

Figure 3. Expression of Abl in Abl/Arg double knockout fibroblasts inhibits cell spreading. (A) Cells expressing vector (V), wild type Abl (Abl), or kinase defective Abl (KD) were harvested for immunoblotting (WB) with indicated antibody. (B) The indicated cells were detached and held in serum-free DMEM for 45 min. After plating on FN (10 μg/ml)-coated coverslides for 20 min, cells were fixed and stained with anti-Abl/Alexa 568–conjugated secondary antibody (red) and Alexa 488–conjugated phalloidin (green). Scale bars, 25 μm. (C) Quantitation of cell spreading in B by measuring cell surface area shown as box plots. Values shown are from at least 100 cells for each sample.

C

the negative effect of Abl was overridden by imatinib (Figure 2D). The ectopic expression of AblT315I inhibited spreading to a similar extent as that of Abl (Figure 2D, vehicle); however, imatinib did not reverse the negative effect of AblT315I (Figure 2D, imatinib). Thus, the stimulatory effect of imatinib on cell spreading is mediated through its inhibition of the Abl tyrosine kinase.

In time-course experiments, we found that the stimulatory effect of imatinib was observed during the first 20 min of plating cells onto a fibronectin-coated surface (Figure 2E, top panel), consistent with previously reported transient activation of Abl kinase activity upon cell adhesion to fibronectin (Lewis *et al.,* 1996; Lewis and Schwartz, 1998). The overproduction of wt-Abl significantly reduced the rate of cell spreading (Figure 2E, bottom panel); however, the addition of imatinib accelerated spreading to a level comparable to that found with imatinib-treated 3T3/vector cells (Figure 2E, compare the two imatinib time courses). Therefore, the negative effect of Abl overproduction on cell spreading requires its kinase activity. We also examined the effect of Abl overproduction on cell adhesion as a function of time and fibronectin concentrations (Figure 2F). Abl overproduction did not affect cell adhesion at the fibronectin concentration tested (0.1 μg/ml~20 μg/ml); neither did it affect cell adhesion between 5 and 120 min after plating on fibronectin (Figure 2F). Thus, Abl kinase is unlikely to interfere with cell spreading by impairing cell adhesion.

### Expression of Abl Kinase in Abl/Arg Double Knockout Mouse Fibroblasts Inhibits Cell Spreading

Previous studies have used fibroblasts derived from *Abl/Arg* double knockout (DKO) mouse embryos to study the effect of Abl kinase on the F-actin cytoskeleton (Woodring *et al.,* 2002; Sini *et al.,* 2004; Leng *et al.,* 2005). The *Abl/Arg* DKO cells are deficient in forming F-actin microspikes when spreading on fibronectin-coated surfaces, but microspikes are formed through Abl reconstitution (Woodring *et al.,* 2002). We expressed murine wt-Abl (type IV) or its kinase-defective mutant (AblKD) in the *Abl/Arg* DKO cells via retroviral-mediated gene transfer and generated polyclonal populations of stable expressers through hygromycin selec-

tion (Figure 3A). As previously reported (Woodring *et al.,* 2002), Abl-reconstituted *Abl/Arg* DKO cells displayed F-actin microspikes when spreading on fibronectin, which was not observed in *Abl/Arg* DKO cells expressing vector or AblKD (Figure 3B). In addition, we found that Abl-reconstituted *Abl/Arg* DKO cells spread slower than those reconstituted with vector or AblKD (Figure 3, B and C). These results further provide genetic evidence for the negative effect of Abl tyrosine kinase on cell spreading.

Imatinib Does Not Affect the GTP Loading of Rac and Rho during Cell Spreading

It is well established that adhesion signals activate Rac-GTP to stimulate lamellipodia extension through actin polymerization (Takenawa and Miki, 2001; Eden *et al.,* 2002; Innocenti *et al.,* 2004). Because imatinib stimulates cell spreading, we determined its effect on Rac-GTP during cell spreading using the Rac-GTP-binding domain of PAK (PBD) as an affinity ligand GST-pulldown assay (Azim *et al.,* 2000). As expected, the Rac-GTP levels were low in detached 3T3 cells but increased rapidly after cell plating on fibronectin (Figure 4, A and B). The addition of imatinib did not affect the Rac-GTP levels during the time frame when it stimulated cell spreading (Figure 4, A and B). In other experiments, we found the GTP-loading of Rac and Cdc42 to be similar between 3T3/vector cells and 3T3/Abl cells that overproduce the Abl protein (not shown). Thus, we were unable to observe an effect of either the endogenous Abl or overproduced Abl on adhesion-induced GTP-loading of Rac.

The levels of Rho-GTP are regulated by cell adhesion as well, but in a different manner from that of Rac-GTP (Ren *et al.,* 1999; Arthur and Burridge, 2001). Detached fibroblasts maintained Rho-GTP. On cell adhesion, the level of Rho-GTP is initially reduced to allow the extension of lamellipodia (Ren *et al.,* 1999; Arthur and Burridge, 2001). The Rho-GTP level then rises during cell spreading to promote the formation of actin stress fibers (Ren *et al.,* 1999). Using the Rho-GTP binding domain of Rhotekin as an affinity ligand (Ren and Schwartz, 2000), we were able to detect the transient reduction in Rho-GTP followed by a restoration of Rho-GTP levels during cell spreading on fibronectin (Figure
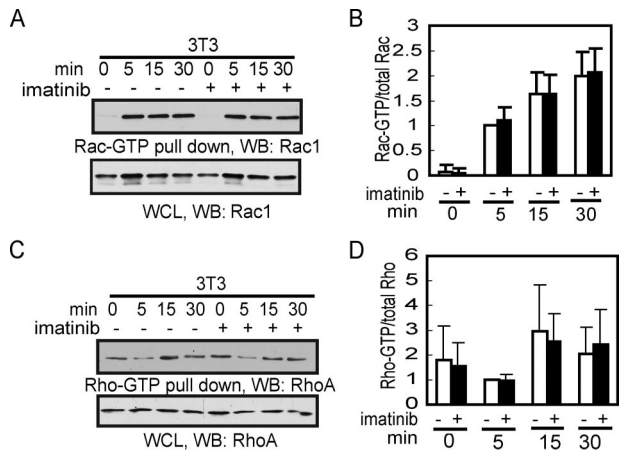
Figure 4. Imatinib does not affect GTP-Rac or GTP-Rho levels during cell spreading. (A) 3T3 fibroblasts were serum starved for 18 h before detachment. Cells were held in serum free DMEM for 30 min and then treated with imatinib (5 μM) or vehicle (0.1% DMSO) for 45 min. Cells were plated on FN-coated dishes for the indicated time and harvested for Rac pull-down with GST-PBD as described in *Materials and Methods*. (B) Quantitation of data in A as described in *Materials and Methods*. The ratio of GST-PBD pull-downed Rac over total Rac of the vehicle-treated 5-min sample was set to 1. Values shown are from three independent experiments. (C) Cells were processed and harvested as in A and Rho was pulled down with GST-RBD (Rho-binding domain of Rhotekin) as described in *Materials and Methods*. (D) Quantitation of GST-RBD pull-down Rho as in B. Values are from three independent experiments.

4, C and D). Again, we were unable to detect any significant effects of imatinib on the Rho-GTP levels (Figure 4, C and D). These results show that imatinib stimulates cell spreading without affecting the overall level of Rac-GTP or Rho-GTP.

Ectopic Expression of RacV12 Does Not Override the Negative Effect of Abl on Cell Spreading

To demonstrate that Abl can inhibit cell spreading despite the activation of Rac, we performed spreading experiments with constitutively active RacV12 (Ridley *et al.*, 1992). We

transfected 3T3/vector or 3T3/Abl cells with plasmids expressing HA-RacV12 and/or GFP. The levels of HA-RacV12 were determined by immunoblotting of whole cell lysate (Figure 5A, top panel), and the levels of HA-RacV12-GTP by GST-PBD pulldown (Figure 5A, middle panel). As expected, ectopic expression of RacV12 stimulated cell spreading (Figure 5B, compare bars 1 and 2, and 4 and 5). However, RacV12-transfected 3T3/Abl cells still spread slower than the RacV12-transfected 3T3/vector cells (Figure 5B, compare bars 2 and 5). The overproduction of Abl did not affect the levels of RacV12 protein, nor did it affect the binding of RacV12 to GST-PBD (Figure 5A, compare lanes 5 and 2). The levels of RacV12 and its binding to GST-PBD were also unaffected by imatinib treatment (Figure 5A, lanes 3 and 6). Nevertheless, imatinib treatment was able to stimulate the spreading of RacV12-transfected 3T3/vector or 3T3/Abl cells to a similar extent (Figure 5B, bars 3 and 6). In addition to cotransfection with GFP, we also examined a GFP-RacV12 fusion protein and observed similar results (Figure 5C). Therefore, ectopic expression of RacV12 does not override the negative effect of Abl on cell spreading.

Abl Kinase-dependent RacV12 Localization to Dorsal Membrane Protrusions

Previous studies have shown that Abl tyrosine kinase stimulates dorsal ruffles in response to growth factor stimulation (Plattner *et al.*, 1999; Sini *et al.*, 2004). Dorsal ruffles are membrane protrusions also stimulated by Rac-mediated actin polymerization (Burridge and Wennerberg, 2004). Given the observations that Abl kinase did not affect the level of RacV12 (Figure 5A) but reduced cell spreading (Figure 5, B and C), we examined whether Abl altered the localization of RacV12 (Figure 6). Among fully spread 3T3/Abl cells, we found GFP-RacV12 localized to dorsal membrane protrusions in ~60% of the cells (Figure 6A, left panels). In the other 40% of fully spread 3T3/Abl cells, GFP-RacV12 was found at the peripheral membranes and cytosolic space (Figure 6A, middle panels), a distribution similar to that in fully spread 3T3/vector cells containing physiological levels of Abl (Figure 6B, left panel). Thus, overproduction of Abl causes dorsal membrane localization of GFP-RacV12 in fully spread cells. This effect of Abl overproduction was completely abrogated by treatment with
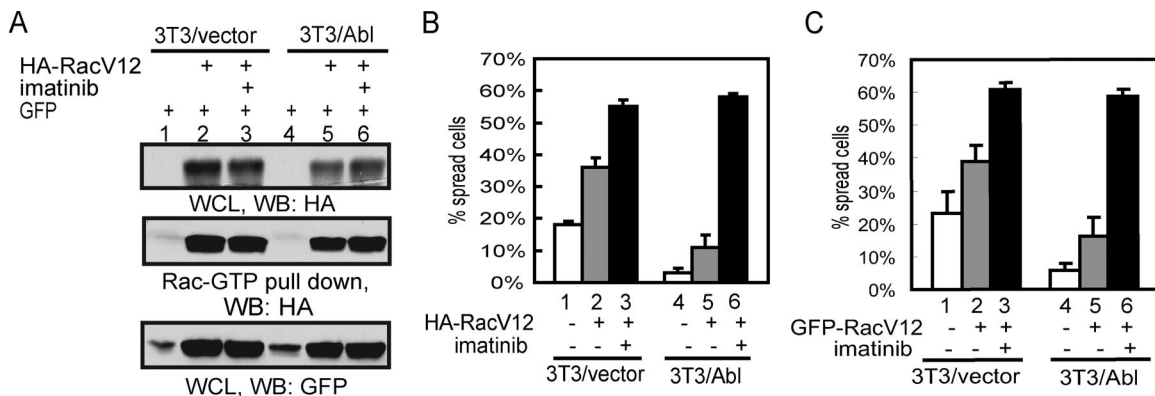
Figure 5. Abl inhibits the spreading of cells expressing RacV12. (A) 3T3 cells were infected with retrovirus encoding vector or Abl, and transfected 48 h later with HA-RacV12 and/or GFP. Transfected cells were detached and held in serum-free DMEM for 30 min, treated with imatinib (5 μM) or vehicle for 45 min and plated on FN (10 μg/ml)-coated plates, collected at 20 min after plating for immunoblotting (WB) and GST-PBD pulldown as described in *Materials and Methods*. (B) Cells prepared as in A were plated on FN (10 μg/ml)-coated coverslips for 20 min, fixed and stained with anti-Abl/Alexa 568–conjugated secondary antibody. In the 3T3/vector sample, GFP-positive cells were evaluated for spreading. In the 3T3/Abl sample, cells that were GFP positive and with higher levels of Abl were scored. At least 100 cells were counted in each sample from three independent experiments. (C) The indicated cells were transfected with GFP-RacV12, treated and cell spreading determined as in B. At least 100 cells were counted in each sample from three independent experiments.

Figure 6. Abl Kinase promotes RacV12 localization to dorsal membrane protrusion. The indicated 3T3/vector or 3T3/Abl cells were transfected with GFP-RacV12 (A and B), GFP-Rac (C), or GFP (D), treated with imatinib (5 μM) or vehicle (0.1% DMSO) and then allowed to spread on FN. Cells were fixed between 60 and 90 min after plating, stained with anti-Abl/Alexa 568–conjugated secondary antibody (red). Images of fully spread cells were captured by deconvolution microscopy. Representative Z sections from the top of the cells are shown: GFP (green), Abl (red) and merge (yellow). Cells with or without dorsal localization of GFP-RacV12, GFP-Rac, or GFP were determined as describe in *Materials and Methods*. (A) GFP-RacV12–transfected 3T3/Abl cells. Left panels, a cell with GFP-positive dorsal membrane protrusions (yellow arrow), representing ~58% of spread cells among 50 cells counted. Middle panels, a cell without GFP-positive dorsal membrane protrusions, representing ~42% of spread cells among 50 cells counted. Right panels, an imatinib-treated GFP-RacV12–transfected 3T3/Abl cell. Of 50 cells examined, ~96% showed GFP signals at the peripheral membrane and in the cytosolic space. Scale bars, 10 μm. (B) GFP-RacV12–transfected 3T3/vector cells. Left panels, a cell with GFP signal at the peripheral membrane and in the cytosolic space, representing 91% of spread cells among 50 cells counted. Right panels, an imatinib treated GFP-RacV12–transfected 3T3/vector cells. Of 50 cells counted, 97% showed GFP signals at the peripheral membrane and in the cytosolic space. Scale bars equal 10 μm. (C) GFP-Rac–transfected 3T3/Abl cells. Left panels, a cell with GFP-positive dorsal membrane protrusions (yellow arrow), representing ~39% of spread cells among 50 cells counted. Middle panels, a cell without GFP-positive dorsal membrane protrusions, representing ~61% of spread cells among 50 cells counted. Right panels, imatinib treated GFP-Rac transfected 3T3/Abl cells. Of 50 cells examined, ~98%

showed GFP signals at the peripheral membrane and in the cytosolic space. Scale bars, 10 μm. (D) GFP transfected 3T3/Abl cells. Left panels, a cell with GFP signal diffusely throughout the cell, representing ~97% of spread cells among 50 counted. Right panels, imatinib treated GFP transfected 3T3/Abl cells. Of 50 cells examined, ~97% showed GFP signals diffusely throughout the cell. Scale bars, 10 μm.
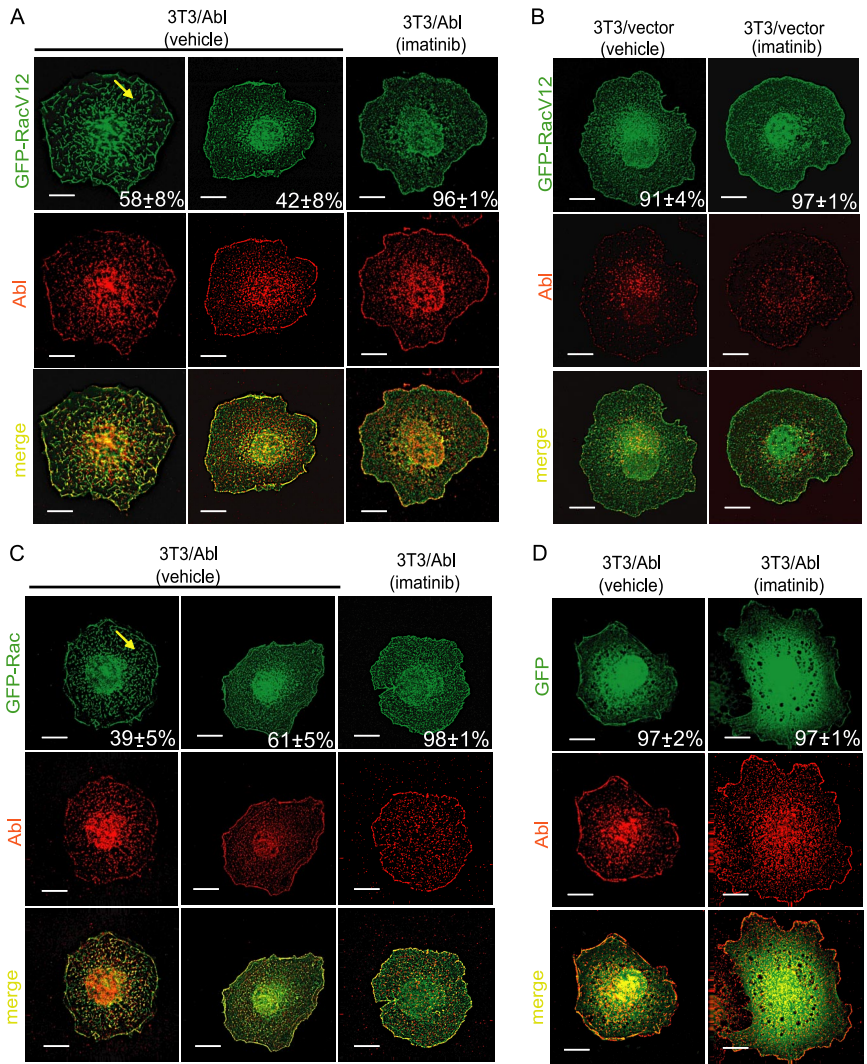
imatinib in that GFP-RacV12 was distributed at the peripheral membranes and cytosolic space in ~96% of fully spread cells (Figure 6A, right panels). We also examined the distribution of GFP-Rac in 3T3/Abl cells. Without imatinib, ~40% of fully spread 3T3/Abl cells showed GFP-Rac in dorsal membrane protrusions, which were less prominent than those found in 3T3 cells expressing GFP-RacV12 (Figure 6C, left panels). With imatinib, virtually none of the GFP-Rac was localized to dorsal membrane protrusions (Figure 6C, right panels). As a control, GFP signal was found at the cell periphery and diffusely in the cytosolic space of, and we did not observe dorsal membrane localization of GFP with or without imatinib fully spread 3T3/Abl cells (Figure 6D). These results showed that Abl tyrosine kinase could sequester Rac at the dorsal membrane, correlating with the formation of dorsal protrusions.

Abl Kinase Prolongs Dorsal Ruffling during Cell Spreading

Activated Rac-GTP stimulates membrane protrusions including ruffles and lamellipodia (Ridley and Hall, 1992). If the Abl-mediated RacV12 localization to dorsal ruffles also applied to the endogenous Rac-GTP, we would expect 3T3/Abl cells to exhibit increased dorsal ruffling relative to their imatinib-treated counterparts. We therefore examined dorsal ruffles, which was scored as F-actin–rich wrinkles on the topside of spreading cells away from the fibronectin-coated surface by deconvolution microscopy (Figure 7, A and B). Immediately after plated on fibronectin-coated coverslides, 3T3/Abl cells displayed dorsal ruffles irrespective of imatinib treatment (small cells, 550–750 μm^2; Figure 7, A and C), indicating that adhesion-induced dorsal ruffles does not require Abl kinase activity. Among the larger and more spread-out 3T3/Abl cells, 70–80% retained dorsal ruffles in the absence of imatinib but only 20–30% retained dorsal ruffles in the presence of imatinib (large cells, 1500–1750 μm^2; Figure 7, B and C).

The observation that overproduction of Abl kinase promoted dorsal ruffles (Figure 7, A–C) prompted us to examine whether endogenous Abl also regulates dorsal ruffling during cell spreading. By scanning electron microscopy, we
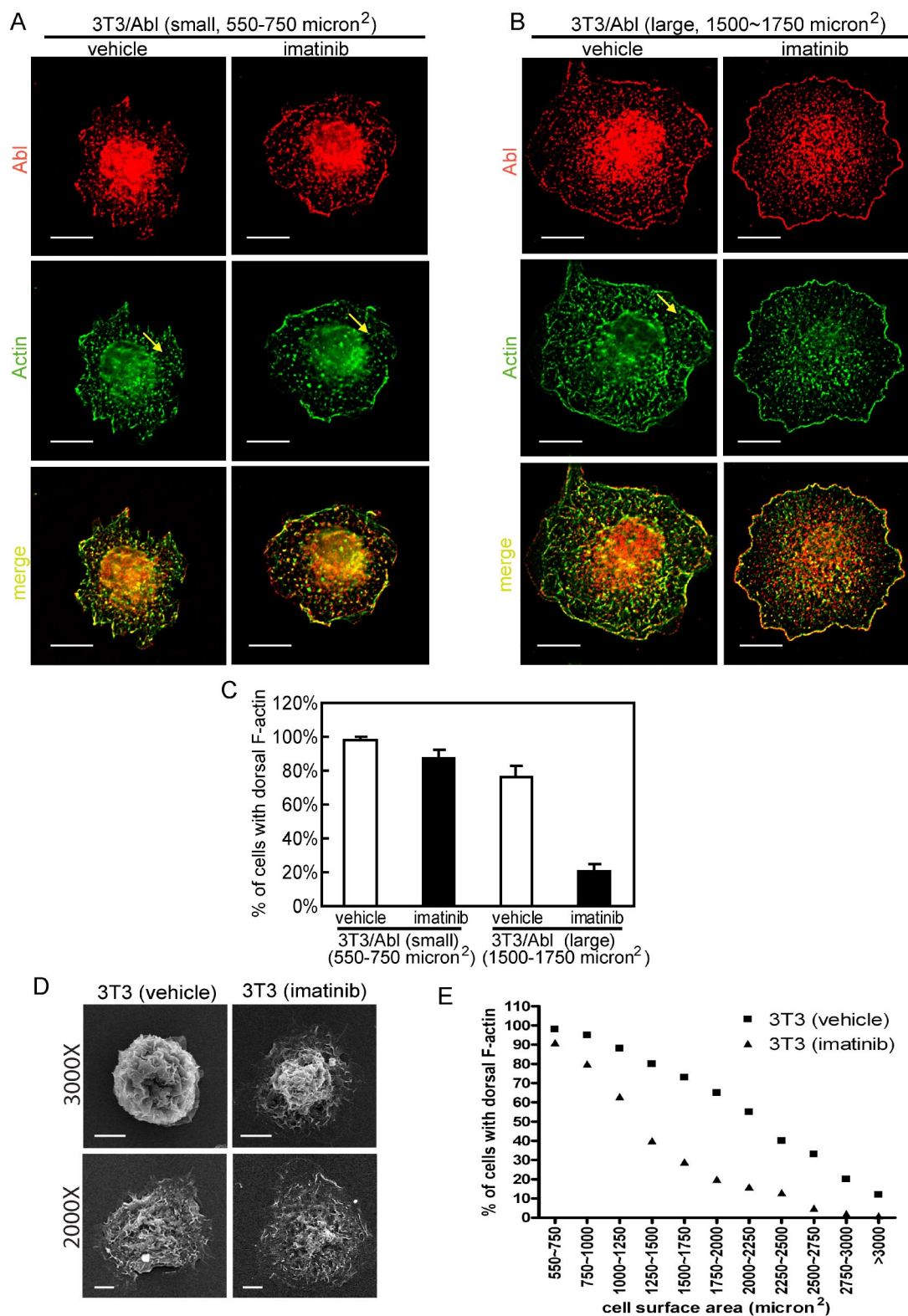
Figure 7. Abl kinase prolongs dorsal ruffling during cell spreading. (A) and (B) 3T3/Abl cells treated with imatinib (5 μM) or vehicle (0.1% DMSO) were allowed to spread on FN (10 μg/ml)-coated coverslides, fixed at 20 or 40 min, stained with anti-Abl/Alexa 568–conjugated secondary antibody (red) and Alexa 488–conjugated phalloidin (green). Z-section images from the top of cells captured by deconvolution microscopy are shown. Yellow arrow points to F-actin–rich dorsal protrusions. (A) A representative image of a small cell (cell area from 550 to 750 μm^2). Scale bars, 10 μm. (B) Representative images of a large cell (cell area from 1500 to 1750 μm^2). Scale bars, 10 μm. (C) Quantitation of cells showing dorsal F-actin ruffles as described in *Materials and Methods*. (D) 3T3 cells treated with imatinib (5 μM) or vehicle (0.1% DMSO) were allowed to spread on FN-coated coverslides and fixed. Images were collected by scanning electronic microscopy (SEM) show dorsal ruffles in vehicle and imatinib treated cells. Scale bars, 5 μm. (E) 3T3 cells treated with imatinib or vehicle as in (D) were fixed at 20 or 40 min

confirmed that fibronectin-induced dorsal ruffling occurred irrespective of imatinib treatment (Figure 7D), consistent with the result that imatinib did not affect fibronectin-induced GTP loading of Rac (Figure 4A), which stimulates membrane protrusions (Ridley and Hall, 1992). We then determined the percentage of cells with dorsal F-actin ruffles as a function of cell area, collecting data at 20 and 40 min after plating cells on fibronectin (Figure 7E). We found an inverse correlation between cell area and dorsal ruffles. Interestingly, this negative correlation was significantly enhanced with imatinib-treated cells (Figure 7E), suggesting imatinib-treated cells lose their dorsal ruffles faster than their untreated counterparts. This result is consistent with the notion that Abl tyrosine kinase maintains dorsal ruffling during cell spreading.

Effects of Crk and Dynamin on Abl-dependent Dorsal Localization of RacV12

To explore the mechanism of Abl kinase-dependent dorsal membrane location of activated Rac, we examined the effect of CrkII. Previous studies have shown CrkII to stimulate cell spreading and migration by activating Rac (Kain and Klemke, 2001; Abassi and Vuori, 2002). Previous studies have also established CrkII to be a substrate of Abl (Feller *et al.,* 1994; Ren *et al.,* 1994) and that tyrosine phosphorylation of CrkII at Y221 leads to an intramolecular SH2-Ptyr interaction that inactivates the CrkII SH2 adaptor function (Rosen *et al.,* 1995). When CrkII was coexpressed with GFP-RacV12 in 3T3/Abl cells, we observed a reduction in the dorsal membrane localization of the GFP signal (Figure 8A). Correspondingly, expression of CrkII stimulated the spreading of 3T3/Abl cells (Figure 8B). The ectopic expression of CrkII did not completely abrogate the effects of imatinib on GFP-RacV12 localization and spreading (Figure 8, A and B). We also examined the effect of CrkII-Y221F mutant. We found that the Y221F mutation did not create a constitutively active CrkII in that it did not reduce Abl-dependent dorsal membrane localization of GFP-RacV12, neither did it stimulate cell spreading (Figure 8B). Furthermore, CrkII-Y221F maintained dorsal localization of GFP-RacV12 in imatinib-treated 3T3/Abl cells (Figure 8A), corresponding to a slower rate of cell spreading (Figure 8B). These results suggest that the interplay between CrkII and Abl may regulate the localization of active Rac and cell spreading.

We also examined the role of dynamin-2 in Abl-dependent dorsal localization of RacV12 because a previous report has shown dynamin-2 to play a role in Rac translocation to the leading edge (Schlunck *et al.,* 2004). The ectopic expression of wt-dynamin-2 did not affect the localization of GFP-RacV12 or the spreading of 3T3/Abl cells (Figure 8, C and D). Expression of a dominant negative dynamin-2-K44A, which has been shown to induce dorsal membrane localization of Rac-GTP and inhibit cell spreading (Schlunck *et al.,* 2004), did not cause a significant further spreading inhibition of 3T3/Abl cells that already spread slowly due to the overproduction of Abl. However, in the presence of dynamin-2-K44A, the spreading stimulatory effect of imatinib was partially abolished (Figure 8D), correlating with sustained dorsal localization of GFP-RacV12 (Figure 8C). These
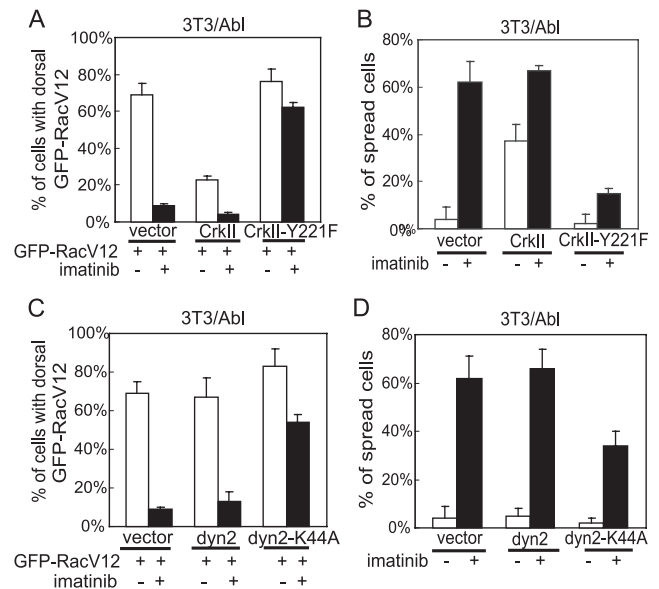
Figure 8. Effects of CrkII and dominant negative dynamin-2 on RacV12 dorsal membrane localization. (A) 3T3/Abl cells were co-transfected with GFP-RacV12 and CrkII, or CrkII-Y221F. Transfected cells were treated with imatinib (5 μM) or vehicle (0.1% DMSO) and allowed to spread on FN (10 μg/ml)-coated coverslides and fixed between 60 and 90 min. Dorsal localization of GFP signals in fully spread cells was scored as in Figure 6. (B) 3T3/Abl cells were cotransfected with GFP and CrkII, or CrkII-Y221F. Transfected cells were treated with imatinib or vehicle and allowed to spread on FN-coated coverslides for 20 min. Percentage of spread cells was determined among at least 100 GFP-positive cells. The values and standard deviations were from three independent experiments. (C) 3T3/Abl cells were cotransfected with GFP-RacV12 and dynamin-2, or dynamin-2-K44A. Transfected cells were treated with imatinib or vehicle and allowed to spread on FN-coated coverslides and fixed between 60 and 90 min. Localization of GFP signals in fully spread cells was scored as in Figure 6. (D) 3T3/Abl cells were cotransfected with GFP and dynamin-2, or dynamin-2-K44A. Transfected cells were treated with imatinib or vehicle and allowed to spread on FN-coated coverslides for 20 min. Percentage of spreading cells was determined as in B.

results suggest that the Abl kinase and the dominant negative dynamin mutant are likely to act through the same or an interdependent mechanism to regulate active Rac localization and cell spreading.

DISCUSSION

Abl Regulates Cell Spreading

We have established that Abl tyrosine kinase regulates cell spreading with several lines of evidences. Expression of Abl, but not its kinase-defective mutant (AblKD), in *Abl/Arg* double knockout cells inhibits cell spreading (Figure 3, B and C). Dimerization-induced activation of Abl-FKBP (but not AblKD-FKBP) or overproduction of Abl exerts a negative effect on 3T3 cell spreading (Figures 1, C–E, and 2D). Conversely, shRNA-mediated Abl knockdown or inhibition of Abl kinase with imatinib stimulates cell spreading, and an imatinib-resistant AblT315I kinase overrides this effect (Figure 2, A, B, and D). Cell spreading is a complex and dynamic process. Using total internal reflection fluorescence (TIRF) microscopy, a previous study has described two modes of spreading: anisotropic and isotropic (Dubin-Thaler *et al.,* 2004). The isotropic spreading, with a higher initial rate of

Figure 7 (cont). after plated on FN-coated coverslides. Individual cells were analyzed for size and dorsal F-actin protrusions as depicted in A and B. Cells were grouped into 11 categories based on size, and in each category, at least 50 cells were counted to determine the percentage of cells with dorsal F-actin ruffles.

area increase and 78% of the cell edge extending, is more prevalent with serum-starved cells (Dubin-Thaler *et al.*, 2004). The Abl kinase is activated by growth factors and by cell adhesion (Lewis *et al.*, 1996; Plattner *et al.*, 1999). We conducted the spreading experiments in serum-free condition that favors isotropic spreading. Although we did not apply TIRF in this study, our results suggest that inhibition of Abl tyrosine kinase further enhance isotropic spreading in serum-starved cells. In other words, the Abl tyrosine kinase may antagonize the isotropic mode or stimulate the anisotropic mode of spreading as indicated by the slower rate of area increase and the prolonged dorsal ruffling during cell spreading with increased Abl activity.

Regulation of Rac-GTP Localization

Rac is activated by cell adhesion to induce lamellipodia formation and thus promotes cell spreading (Clark *et al.*, 1998; Price *et al.*, 1998; Vidali *et al.*, 2006). Although Abl has been shown to enhance growth-factor–stimulated Rac-GTP levels (Sini *et al.*, 2004), we have found that Abl kinase does not affect the GTP loading of Rac stimulated by cell adhesion to fibronectin (Figure 4, A and B). We also show that Abl kinase activity is not required for fibronectin to initiate dorsal ruffles (Figure 7, A, C, and D); instead, Abl kinase prolongs dorsal ruffling during cell spreading (Figure 7, B, C, and E). Furthermore, Abl inhibits the spreading of cells that express the activated Rac mutant, RacV12 (Figure 5, B and C), correlating with an Abl kinase-dependent localization of RacV12 to the dorsal membrane protrusions (Figure 6). These results suggest that Abl tyrosine kinase may regulate the partitioning of Rac-GTP to favor dorsal ruffles and thus reducing the pool of Rac-GTP for lamellipodia extension to inhibit lamellipodia extension.

The membrane localization of Rac-GTP is stimulated by cell adhesion signals (del Pozo *et al.*, 2000, 2002, 2004). Targeting of Rac-GTP to cholesterol-enriched membrane microdomains is required for Rac-GTP to activate its downstream effectors (del Pozo *et al.*, 2004). Results from this study suggest that the distribution of Rac-GTP within the plasma membrane may be further regulated through integrin-dependent activation of Abl tyrosine kinase. Shlunck *et al.* (2004) have proposed that Rac-GTP is translocated through a dynamin-dependent endocytosis pathway to the basal membrane that contacts the ECM and thus fueling the continuous extension of the lamellipodia during cell spreading. This notion is consistent with the findings that Rac-GTP is distributed in the plasma membrane and the cytoplasm (Del Pozo *et al.*, 2002).

We have replicated the result of Shlunck *et al.* (2004), showing that the dominant negative dynamin-2-K44A mutant inhibits the spreading of 3T3 cells (not shown). With 3T3/Abl cells that already spread slower because of the overproduction of Abl, dynamin-2-K44A does not further reduce cell spreading (Figure 8D). However, the stimulatory effect of Abl kinase inhibitor imatinib is stunted in 3T3/Abl cells expressing dynamin-2-K44A (Figure 8D). This result suggests that Abl either acts upstream or in parallel with dynamin to regulate RacV12 localization to the dorsal membrane. A recent report has shown that the Abl tyrosine kinase can inhibit the endocytosis of activated EGF receptor (Tanos and Pendergast, 2006). It is conceivable that Abl tyrosine kinase may prevent the endocytosis of Rac-GTP–containing lipid domain and thus reducing the rate and/or frequency of lamellipodia extension on the fibronectin matrix. The precise mechanism for how Abl tyrosine kinase sequesters Rac-GTP at the dorsal location will await further investigation.

Role of Abl Substrates

We have established that the negative effect of Abl on cell spreading requires its tyrosine kinase activity. The Abl tyrosine kinase phosphorylates a number of proteins that have been implicated in the regulation of F-actin polymerization (Woodring *et al.*, 2003). These include the Crk-family, the Dok-family, the p130Cas-family of adaptor proteins, and the components of the WAVE complex (Dai and Pendergast, 1995; Mayer *et al.*, 1995; Kain and Klemke, 2001; Woodring *et al.*, 2004; Leng *et al.*, 2005). Tyrosine phosphorylation of Dok-1 by Abl has been shown to promote F-actin microspikes during cell spreading (Woodring *et al.*, 2004). We also observed Abl-dependent formation of microspikes in Abl-reconstituted *Abl/Arg* DKO cells (Figure 3B). Despite increased Dok-1 phosphorylation, we did not observe F-actin microspikes in spreading 3T3 cells overexpressing Abl either in the presence or absence of imatinib (Figure 2, B and C). These observations suggest that microspike formation is not necessary for Abl to inhibit cell spreading; additionally, neither wt-Dok-1 or Dok-1 phosphorylation site mutant, Dok-1 Y361F (Woodring *et al.*, 2004) reverses Abl-mediated inhibition of cell spreading (data not shown), suggesting Dok-1 phosphorylation by Abl may not be sufficient to inhibit cell spreading. Nevertheless, Dok-1 and WAVE2 phosphorylation by Abl is likely to stimulate actin polymerization at the dorsal membrane (Woodring *et al.*, 2004; Stuart *et al.*, 2006), which may contribute to the sequestration of Rac-GTP.

Our results suggest that Abl-dependent phosphorylation of Crk is involved in the regulation of Rac localization and cell spreading. During cell spreading on fibronectin, CrkII stimulates membrane localization of Rac-GTP without affecting the overall levels of Rac-GTP (Abassi and Vuori, 2002). We have found that overproduction of CrkII reduces the dorsal membrane localization of RacV12 and partially reduces the spreading defect of 3T3/Abl cells (Figure 8, A and B). By contrast, we found that CrkII-Y221F, which is not phosphorylated by Abl (Feller *et al.*, 1994), does not stimulate the spreading of 3T3/Abl cells (Figure 8B). Thus, mutation of Y221 does not create a constitutively active CrkII for cell spreading; rather, it abolishes the spreading-stimulatory activity of CrkII. Abassi and Vuori (2002) have shown that CrkII stimulates the membrane targeting of RacV12 and that CrkII-Y221F was defective in this activity . We have found that expression of CrkII-Y221F maintains the dorsal membrane localization of Rac-GTP in 3T3/Abl cells (Figure 8A), suggesting that this mutant is not defective in targeting Rac-GTP to the membrane, but rather, it preferentially target Rac-GTP to dorsal membrane ruffles. Treatment with imatinib did not reverse the dorsal sequestration of RacV12 in cells expressing CrkII-Y221F (Figure 8A). These results suggest that the interplay between Abl and CrkII is involved in the regulation of Rac-GTP localization and thus cell spreading. However, this interaction is likely to be modulated by other mechanisms to account for the net negative effect of Abl kinase on cell spreading.

REFERENCES

Abassi, Y. A., and Vuori, K. (2002). Tyrosine 221 in Crk regulates adhesion-dependent membrane localization of Crk and Rac and activation of Rac signaling. EMBO J. *21*, 4571–4582.

Arthur, W. T., and Burridge, K. (2001). RhoA inactivation by p190RhoGAP regulates cell spreading and migration by promoting membrane protrusion and polarity. Mol. Biol. Cell *12*, 2711–2720.

Azim, A. C., Barkalow, K. L., and Hartwig, J. H. (2000). Determination of GTP loading on Rac and Cdc42 in platelets and fibroblasts. Methods Enzymol. *325*, 257–263.

Brummelkamp, T. R., Bernards, R., and Agami, R. (2002). A system for stable expression of short interfering RNAs in mammalian cells. Science *296*, 550–553.

Burridge, K., and Wennerberg, K. (2004). Rho and Rac take center stage. Cell *116*, 167–179.

Clackson, T. *et al.* (1998). Redesigning an FKBP-ligand interface to generate chemical dimerizers with novel specificity. Proc. Natl. Acad. Sci. USA *95*, 10437–10442.

Clark, E. A., King, W. G., Brugge, J. S., Symons, M., and Hynes, R. O. (1998). Integrin-mediated signals regulated by members of the rho family of GTPases. J. Cell Biol. *142*, 573–586.

Cory, G. O., and Ridley, A. J. (2002). Cell motility: braking WAVEs. Nature *418*, 732–733.

Dai, Z., and Pendergast, A. M. (1995). Abi-2, a novel SH3-containing protein interacts with the c-Abl tyrosine kinase and modulates c-Abl transforming activity. Genes Dev. *9*, 2569–2582.

del Pozo, M. A., Alderson, N. B., Kiosses, W. B., Chiang, H. H., Anderson, R. G., and Schwartz, M. A. (2004). Integrins regulate Rac targeting by internalization of membrane domains. Science *303*, 839–842.

Del Pozo, M. A., Kiosses, W. B., Alderson, N. B., Meller, N., Hahn, K. M., and Schwartz, M. A. (2002). Integrins regulate GTP-Rac localized effector interactions through dissociation of Rho-GDI. Nat. Cell Biol. *4*, 232–239.

del Pozo, M. A., Price, L. S., Alderson, N. B., Ren, X. D., and Schwartz, M. A. (2000). Adhesion to the extracellular matrix regulates the coupling of the small GTPase Rac to its effector PAK. EMBO J. *19*, 2008–2014.

Druker, B. J., Tamura, S., Buchdunger, E., Ohno, S., Segal, G. M., Fanning, S., Zimmermann, J., and Lydon, N. B. (1996). Effects of a selective inhibitor of the Abl tyrosine kinase on the growth of Bcr-Abl positive cells. Nat. Med. *2*, 561–566.

Dubin-Thaler, B. J., Giannone, G., Dobereiner, H. G., and Sheetz, M. P. (2004). Nanometer analysis of cell spreading on matrix-coated surfaces reveals two distinct cell states and STEPs. Biophys. J. *86*, 1794–1806.

Eden, S., Rohatgi, R., Podtelejnikov, A. V., Mann, M., and Kirschner, M. W. (2002). Mechanism of regulation of WAVE1-induced actin nucleation by Rac1 and Nck. Nature *418*, 790–793.

Fan, P. D., and Goff, S. P. (2000). Abl interactor 1 binds to sos and inhibits epidermal growth factor- and v-Abl-induced activation of extracellular signal-regulated kinases. Mol. Cell Biol. *20*, 7591–7601.

Feller, S. M., Knudsen, B., and Hanafusa, H. (1994). c-Abl kinase regulates the protein binding activity of c-Crk. EMBO J. *13*, 2341–2351.

Frasca, F., Vigneri, P., Vella, V., Vigneri, R., and Wang, J. Y. (2001). Tyrosine kinase inhibitor STI571 enhances thyroid cancer cell motile response to Hepatocyte Growth Factor. Oncogene *20*, 3845–3856.

Gorre, M. E., Mohammed, M., Ellwood, K., Hsu, N., Paquette, R., Rao, P. N., and Sawyers, C. L. (2001). Clinical resistance to STI-571 cancer therapy caused by BCR-ABL gene mutation or amplification. Science *293*, 876–880.

Hall, A., and Nobes, C. D. (2000). Rho GTPases: molecular switches that control the organization and dynamics of the actin cytoskeleton. Philos. Trans. R. Soc. Lond. B Biol. Sci. *355*, 965–970.

Hantschel, O., Wiesner, S., Guttler, T., Mackereth, C. D., Rix, L. L., Mikes, Z., Dehne, J., Gorlich, D., Sattler, M., and Superti-Furga, G. (2005). Structural basis for the cytoskeletal association of Bcr-Abl/c-Abl. Mol. Cell *19*, 461–473.

Innocenti, M., Zucconi, A., Disanza, A., Frittoli, E., Areces, L. B., Steffen, A., Stradal, T. E., Di Fiore, P. P., Carlier, M. F., and Scita, G. (2004). Abi1 is essential for the formation and activation of a WAVE2 signalling complex. Nat. Cell Biol. *6*, 319–327.

Kain, K. H., and Klemke, R. L. (2001). Inhibition of cell migration by Abl family tyrosine kinases through uncoupling of Crk-CAS complexes. J. Biol. Chem. *276*, 16185–16192.

Koleske, A. J., Gifford, A. M., Scott, M. L., Nee, M., Bronson, R. T., Miczek, K. A., and Baltimore, D. (1998). Essential roles for the Abl and Arg tyrosine kinases in neurulation. Neuron *21*, 1259–1272.

Leng, Y., Zhang, J., Badour, K., Arpaia, E., Freeman, S., Cheung, P., Siu, M., and Siminovitch, K. (2005). Abelson-interactor-1 promotes WAVE2 membrane translocation and Abelson-mediated tyrosine phosphorylation required for WAVE2 activation. Proc. Natl. Acad. Sci. USA *102*, 1098–1103.

Lewis, J. M., Baskaran, R., Taagepera, S., Schwartz, M. A., and Wang, J. Y. (1996). Integrin regulation of c-Abl tyrosine kinase activity and cytoplasmic-nuclear transport. Proc. Natl. Acad. Sci. USA *93*, 15174–15179.

Lewis, J. M., and Schwartz, M. A. (1998). Integrins regulate the association and phosphorylation of paxillin by c-Abl. J. Biol. Chem. *273*, 14225–14230.

Mayer, B. J., Hirai, H., and Sakai, R. (1995). Evidence that SH2 domains promote processive phosphorylation by protein-tyrosine kinases. Curr. Biol. *5*, 296–305.

McWhirter, J. R., and Wang, J. Y. (1993). An actin-binding function contributes to transformation by the Bcr-Abl oncoprotein of Philadelphia chromosome-positive human leukemias. EMBO J. *12*, 1533–1546.

Plattner, R., Kadlec, L., DeMali, K. A., Kazlauskas, A., and Pendergast, A. M. (1999). c-Abl is activated by growth factors and Src family kinases and has a role in the cellular response to PDGF. Genes Dev. *13*, 2400–2411.

Price, L. S., Leng, J., Schwartz, M. A., and Bokoch, G. M. (1998). Activation of Rac and Cdc42 by integrins mediates cell spreading. Mol. Biol. Cell *9*, 1863–1871.

Ren, R., Ye, Z. S., and Baltimore, D. (1994). Abl protein-tyrosine kinase selects the Crk adapter as a substrate using SH3-binding sites. Genes Dev. *8*, 783–795.

Ren, X. D., Kiosses, W. B., and Schwartz, M. A. (1999). Regulation of the small GTP-binding protein Rho by cell adhesion and the cytoskeleton. EMBO J. *18*, 578–585.

Ren, X. D., and Schwartz, M. A. (2000). Determination of GTP loading on Rho. Methods Enzymol. *325*, 264–272.

Renshaw, M. W., Lea-Chou, E., and Wang, J. Y. (1996). Rac is required for v-Abl tyrosine kinase to activate mitogenesis. Curr. Biol. *6*, 76–83.

Ridley, A. J., Allen, W. E., Peppelenbosch, M., and Jones, G. E. (1999). Rho family proteins and cell migration. Biochem. Soc. Symp. *65*, 111–123.

Ridley, A. J., and Hall, A. (1992). Distinct patterns of actin organization regulated by the small GTP-binding proteins Rac and Rho. Cold Spring Harb. Symp. Quant. Biol. *57*, 661–671.

Ridley, A. J., Paterson, H. F., Johnston, C. L., Diekmann, D., and Hall, A. (1992). The small GTP-binding protein rac regulates growth factor-induced membrane ruffling. Cell *70*, 401–410.

Ridley, A. J., Schwartz, M. A., Burridge, K., Firtel, R. A., Ginsberg, M. H., Borisy, G., Parsons, J. T., and Horwitz, A. R. (2003). Cell migration: integrating signals from front to back. Science *302*, 1704–1709.

Rosen, M. K., Yamazaki, T., Gish, G. D., Kay, C. M., Pawson, T., and Kay, L. E. (1995). Direct demonstration of an intramolecular SH2-phosphotyrosine interaction in the Crk protein. Nature *374*, 477–479.

Schindler, T., Bornmann, W., Pellicena, P., Miller, W. T., Clarkson, B., and Kuriyan, J. (2000). Structural mechanism for STI-571 inhibition of abelson tyrosine kinase. Science *289*, 1938–1942.

Schlunck, G., Damke, H., Kiosses, W. B., Rusk, N., Symons, M. H., Waterman-Storer, C. M., Schmid, S. L., and Schwartz, M. A. (2004). Modulation of Rac localization and function by dynamin. Mol. Biol. Cell *15*, 256–267.

Schwartzberg, P. L., Stall, A. M., Hardin, J. D., Bowdish, K. S., Humaran, T., Boast, S., Harbison, M. L., Robertson, E. J., and Goff, S. P. (1991). Mice homozygous for the ablm1 mutation show poor viability and depletion of selected B and T cell populations. Cell *65*, 1165–1175.

Sini, P., Cannas, A., Koleske, A. J., Di Fiore, P. P., and Scita, G. (2004). Abl-dependent tyrosine phosphorylation of Sos-1 mediates growth-factor-induced Rac activation. Nat. Cell Biol. *6*, 268–274.

Small, J. V., Stradal, T., Vignal, E., and Rottner, K. (2002). The lamellipodium: where motility begins. Trends Cell Biol. *12*, 112–120.

Smith, K. M., and Van Etten, R. A. (2001). Activation of c-Abl kinase activity and transformation by a chemical inducer of dimerization. J. Biol. Chem. *276*, 24372–24379.

Soderling, S. H., and Scott, J. D. (2006). WAVE signalling: from biochemistry to biology. Biochem. Soc. Trans. *34*, 73–76.

Steffen, A., Rottner, K., Ehinger, J., Innocenti, M., Scita, G., Wehland, J., and Stradal, T. E. (2004). Sra-1 and Nap1 link Rac to actin assembly driving lamellipodia formation. EMBO J. *23*, 749–759.

Stradal, T. E., Rottner, K., Disanza, A., Confalonieri, S., Innocenti, M., and Scita, G. (2004). Regulation of actin dynamics by WASP and WAVE family proteins. Trends Cell Biol. *14*, 303–311.

Stuart, J. R., Gonzalez, F. H., Kawai, H., and Yuan, Z. M. (2006). c-Abl interacts with the WAVE2 signaling complex to induce membrane ruffling and cell spreading. J. Biol. Chem. *281*, 31290–31297.

Suetsugu, S., and Takenawa, T. (2003). Regulation of cortical actin networks in cell migration. Int. Rev. Cytol. *229*, 245–286.

Takenawa, T., and Miki, H. (2001). WASP and WAVE family proteins: key molecules for rapid rearrangement of cortical actin filaments and cell movement. J. Cell Sci. *114*, 1801–1809.

Tanos, B., and Pendergast, A. M. (2006). Abl tyrosine kinase regulates endocytosis of the epidermal growth factor receptor. J. Biol. Chem. *281*, 32714–32723.

Tybulewicz, V. L., Crawford, C. E., Jackson, P. K., Bronson, R. T., and Mulligan, R. C. (1991). Neonatal lethality and lymphopenia in mice with a homozygous disruption of the c-abl proto-oncogene. Cell *65*, 1153–1163.

Van Etten, R. A., Jackson, P. K., Baltimore, D., Sanders, M. C., Matsudaira, P. T., and Janmey, P. A. (1994). The COOH terminus of the c-Abl tyrosine kinase contains distinct F- and G-actin binding domains with bundling activity. J. Cell Biol. *124*, 325–340.

Vella, V., Zhu, J., Frasca, F., Li, C. Y., Vigneri, P., Vigneri, R., and Wang, J. Y. (2003). Exclusion of c-Abl from the nucleus restrains the p73 tumor suppression function. J. Biol. Chem. *278*, 25151–25157.

Vidali, L., Chen, F., Cicchetti, G., Ohta, Y., and Kwiatkowski, D. J. (2006). Rac1-null mouse embryonic fibroblasts are motile and respond to platelet-derived growth factor. Mol. Biol. Cell *17*, 2377–2390.

Wang, J. Y. (2000). Regulation of cell death by the Abl tyrosine kinase. Oncogene *19*, 5643–5650.

Welch, P. J., and Wang, J. Y. (1995). Abrogation of retinoblastoma protein function by c-Abl through tyrosine kinase-dependent and -independent mechanisms. Mol. Cell Biol. *15*, 5542–5551.

Wiesner, S., Hantschel, O., Mackereth, C. D., Superti-Furga, G., and Sattler, M. (2005). NMR Assignment Reveals an alpha-Helical Fold for the F-Actin Binding Domain of Human Bcr-Abl/c-Abl. J. Biomol. NMR *32*, 335.

Woodring, P. J., Hunter, T., and Wang, J. Y. (2001). Inhibition of c-Abl tyrosine kinase activity by filamentous actin. J. Biol. Chem. *276*, 27104–27110.

Woodring, P. J., Hunter, T., and Wang, J. Y. (2003). Regulation of F-actin-dependent processes by the Abl family of tyrosine kinases. J. Cell Sci. *116*, 2613–2626.

Woodring, P. J., Hunter, T., and Wang, J. Y. (2005). Mitotic phosphorylation rescues Abl from F-actin-mediated inhibition. J. Biol. Chem. *280*, 10318–10325.

Woodring, P. J., Litwack, E. D., O'Leary, D. D., Lucero, G. R., Wang, J. Y., and Hunter, T. (2002). Modulation of the F-actin cytoskeleton by c-Abl tyrosine kinase in cell spreading and neurite extension. J. Cell Biol. *156*, 879–892.

Woodring, P. J. *et al.* (2004). c-Abl phosphorylates Dok1 to promote filopodia during cell spreading. J. Cell Biol. *165*, 493–503.

Zhu, J., and Wang, J. Y. (2004). Death by Abl: a matter of location. Curr. Top. Dev. Biol. *59*, 165–192.